

A Coupled Polarization-Matrix Inversion and Iteration Approach for Accelerating the Dipole Convergence in a Polarizable Potential Function[†]

Wangshen Xie, Jingzhi Pu, and Jiali Gao*

Department of Chemistry, Digital Technology Center and Supercomputing Institute, University of Minnesota, Minneapolis Minnesota 55455

Received: October 9, 2008; Revised Manuscript Received: November 12, 2008

A coupled polarization-matrix inversion and iteration (CPII) method is described to achieve and accelerate the convergence of induced dipoles for condensed phase systems employing polarizable intermolecular potential functions (PIPF). The present PIPF is based on the Thole interaction dipole model in which all atomic pair interactions are considered, including those that are directly bonded covalently. Although induced dipoles can be obtained both by inverting a $3N \times 3N$ polarization-matrix where N is the number of polarizable sites, or by a direct iterative approach, the latter approach is more efficient computationally for large systems in molecular dynamics simulations. It was found that induced dipole moments failed to converge in the direct iterative approach if 1–2, 1–3, and 1–4 intramolecular interactions are included in the Thole model. However, it is necessary to include all intramolecular interactions in the Thole model to yield the correct molecular anisotropic polarizability tensor. To solve this numerical stability problem, we reformulated the Thole interaction dipole model in terms of molecular block matrices, which naturally leads to a coupled, preconditioning algorithm that involves a polarization-matrix inversion term to account for intramolecular interactions, and an iterative procedure to incorporate the mutual polarization effects between different molecules. The CPII method is illustrated by applying to cubic boxes of water and NMA molecules as well as an alanine pentapeptide configuration, and it was shown that the CPII method can achieve convergence for the dipole induction polarization rapidly in all cases, whereas the direct iterative approach failed to reach convergence in these cases. In addition, the CPII reduces the overall computational costs by decreasing the number of iteration steps in comparison with the direct iteration approach in which intramolecular bonded interactions are excluded to ensure that induced dipole convergence is obtained.

1. Introduction

A major current effort to improve the accuracy of molecular mechanics force fields for biomolecular simulations is the incorporation of explicit polarization terms in the fixed-charge, pairwise potentials.¹ The most common approach for treating polarization effects is to include an atomic induction term that depends on the instantaneous electric field from the permanent charges and induced dipoles of the rest of the system.^{2–11} However, just as partial atomic charges are not uniquely defined and are not experimental observables, nor are atomic polarizabilities. Of course, the total molecular polarization is well-defined, and this gives rise to a variety of formulations for estimating the polarization energy.¹ Three such approaches have been incorporated into the CHARMM force field, as well as in other programs, including the fluctuating charge model,^{12–16} the drude oscillator representation,^{17–22} and the Thole interaction dipole (TID) method.^{9,10,23–26} In other applications, a mixture of these methods or the inclusion of high-order multipole terms have been adopted,^{27–30} and a fully quantum mechanical model, called explicit polarization (X-pol) theory, has been developed.^{31–36} Our goal is to incorporate the TID model²³ into the CHARMM force field³⁷ by making adjustments to the nonbonded interaction terms, and at the same time, by minimizing the need for reparametrization of the internal bonding terms.²⁶ Because of the mutual dependence of many-body polarization effects, the speed of induced-

dipole convergence is a critical issue both for computational efficiency and for conservation of energy in molecular dynamics simulations.^{5,8} In this paper, we describe a coupled, preconditioning polarization-matrix inversion and iteration (CPII) method to accelerate the induced dipole convergence of polarizable intermolecular potential functions (PIPF).^{9,10,26}

A particularly attractive feature of the Thole interaction dipole model is that the anisotropic molecular polarizability can be obtained in good accord with experiment even when isotropic atomic polarizabilities are used.²³ Furthermore, as demonstrated by Thole and later by van Duijnen and co-workers,^{23,24} the isotropic atomic polarizabilities are dependent mainly on the atomic number with negligible variations due to its bonding environment. For example, a single atomic polarizability is sufficient for carbon atom, irrespective to its presence in hydrocarbon compounds, a carbonyl group, or other functional groups. Consequently, it makes force-field parametrization especially simple and computationally efficient since only the diagonal terms of the atomic polarizability tensor are required for atoms in the molecule in which all atomic polarizabilities interact with each other.^{23,24,38} The molecular anisotropy arises from the pair interactions between induced dipoles at a given instantaneous geometry during a dynamics simulation.

There are four main computational algorithms to obtain converged induced dipoles. The most widely used scheme is an iterative approach in which the induced dipoles from the previous iteration step are used to estimate a set of new induced dipoles until self-consistency.³ The direct dipole iterative

[†] Part of the “Max Wolfsberg Festschrift”.

* Corresponding author.

approach is computationally efficient and can yield induced dipoles at any desired accuracy if one does not encounter numerical instability. The second approach is to obtain the induced dipole moments exactly by solving the coupled linear equations of dipolar polarization.^{3,8} The advantage of this technique is that it does not suffer from convergence errors, but the shortcoming is that its computational costs are high because one needs to invert the interaction matrix. For large molecular systems, it is not practical to use the matrix inversion algorithm in molecular dynamics simulations. Third, a predictor-corrector scheme has been described in which iteration is completely avoided with error of the second order with respect to the time step.³⁹ Finally, the induced dipoles can be treated as independent degrees of freedom and its convergence can be propagated by an extended Lagrangian dynamics method.⁵ However, in this case, induced dipoles are not self-consistently converged and it is difficult to control energy transfer between fast (dipole) and slow (nucleus) degrees of freedom.

When all intramolecular polarizations are explicitly taken into account including covalently bonded atom pairs, the short-range interactions between induced point dipoles are usually severely scaled as seen in the TID model²³ where the damping function used to scale the interaction is very short ranged. However, we still observed severe convergence difficulties using the direct iterative approach for obtaining induced dipoles. This appears to be mainly due to numerical instability in the iterative process since all atom pairs are beyond the range of the so-called polarization catastrophe distance,²³ and it is possible to obtain the exact induced-dipoles by matrix inversion. Although we have also implemented the extended Lagrangian dynamics technique into the CHARMM program⁴⁰ for the TID model, it is useful to have an option to carry out molecular dynamics simulations employing converged induced dipoles. In this paper, we describe a coupled polarization matrix-inversion for intramolecular polarization and a self-consistent iterative procedure for intermolecular interactions to achieve rapid convergence.

This paper is organized as follows: in section II we will briefly outline the algorithm used to calculate induced dipoles and describe the dipole convergence problem using the iterative method; section III will derive a method called the coupled polarization-matrix inversion and iteration (CPII) method to solve this problem; section IV will discuss the major findings from the CPII method; and finally, concluding remarks are given in section V.

II. Point Dipole Model

We consider a system of N interacting sites (atoms), consisting of static (permanent) point charges and polarizable centers on which point dipoles are induced in response to the instantaneous electric field at these sites. Assuming linear response, the induced dipole at center i , $\bar{\mu}_i$, is proportional to the total electric field at that position \bar{E}_i^{tot} .^{23,38} If we arrange all induced dipoles as a column vector $\bar{\mu}$, we have

$$\bar{\mu} = \alpha \cdot \bar{E}^{\text{tot}} \quad (1)$$

where \bar{E}^{tot} is a column vector of the total electric field, and α is a block-diagonal matrix of polarizability tensors for the N polarizable sites:

$$\alpha = \begin{pmatrix} \alpha_1 & 0 & \cdots & 0 \\ 0 & \alpha_2 & \cdots & 0 \\ \cdots & \cdots & \cdots & \cdots \\ 0 & 0 & \cdots & \alpha_N \end{pmatrix} \quad (2)$$

The total electric field, \bar{E}^{tot} , has two contributing components, due to the permanent partial charges (\bar{E}^{o}), and from the induced dipoles at different sites (\bar{E}^{ind}):

$$\bar{E}^{\text{tot}} = \bar{E}^{\text{o}} + \bar{E}^{\text{ind}} \quad (3)$$

The permanent and induced electric fields are written in terms of the first-order and the second-order interaction tensor, respectively:

$$\bar{E}^{\text{o}} = \mathbf{T}_{(1)}^{\text{tot}} \cdot \mathbf{Q} \quad (4)$$

where \mathbf{Q} is a column vector of N partial atomic charges, and

$$\bar{E}^{\text{ind}} = \mathbf{T}_{(2)}^{\text{tot}} \cdot \bar{\mu} \quad (5)$$

In eqs 4 and 5, the total first- and second-order interaction matrices, $\mathbf{T}_{(n)}^{\text{tot}}$, ($n = 1, 2$), are arranged as follows

$$\mathbf{T}_{(n)}^{\text{tot}} = \begin{pmatrix} \mathbf{0} & \mathbf{T}_{(n)}^{12} & \cdots & \mathbf{T}_{(n)}^{1N} \\ \mathbf{T}_{(n)}^{21} & \mathbf{0} & \cdots & \mathbf{T}_{(n)}^{2N} \\ \cdots & \cdots & \cdots & \cdots \\ \mathbf{T}_{(n)}^{N1} & \mathbf{T}_{(n)}^{N2} & \cdots & \mathbf{0} \end{pmatrix} \quad (6)$$

In eq 6, $\mathbf{T}_{(n)}^{ij}$ is the n th-order interaction tensor between interaction sites i and j , which is a vector for the first-order term in eq 4, and a 3×3 matrix for the second-order term in eq 5. Thus, the dimension for $\mathbf{T}_{(1)}^{\text{tot}}$ is $3N \times N$ and that for $\mathbf{T}_{(2)}^{\text{tot}}$ is $3N \times 3N$. In general, the n th-order interaction tensor between interaction sites i and j is a matrix of order $(3)^n$, and its matrix elements are defined as the n th sequential derivative operations over the *zeroth* interaction tensor:

$$T_{\alpha\beta\gamma\dots\omega}^{ij} = \nabla_{\alpha}^i \nabla_{\beta}^i \nabla_{\gamma}^i \cdots \nabla_{\omega}^i T^j \quad (7)$$

where the subscripts ($\alpha, \beta, \gamma, \dots, \omega$) specify a Cartesian coordinate (x_i, y_i, z_i) of interaction site i , and $T^j = 1/r_{ij}$ with r_{ij} being the distance from interaction sites i to interaction site j , which is the *zeroth* interaction tensor.^{26,29,30}

It should also be stressed that a restriction is made in constructing the first-order interaction vector $\mathbf{T}_{(1)}^{\text{tot}}$; atom pairs that are directly chemically bonded (1–2 pair) or that are separated by two consecutive bonds (1–3 pair) are excluded, i.e., the permanent atomic partial charges due to 1–2 and 1–3 atom pairs do not contribute to the dipolar polarization of polarizable sites within the same molecule (eq 4). In contrast the second-order dipole interaction tensor $\mathbf{T}_{(2)}^{\text{tot}}$ does include all intramolecular atomic pairs. Thus, short-range intramolecular interactions are accounted for in the mutual dipolar polarization, including induced dipole–induced dipole interactions. We note that a similar convention is used in the Drude oscillator model in CHARMM.²⁰

With the above definition, eq 1 can be rewritten as follows

$$\bar{\mu} = \alpha \cdot (\bar{E}^{\text{o}} + \mathbf{T}_{(2)}^{\text{tot}} \cdot \bar{\mu}) \quad (8)$$

There are several ways of solving these coupled linear equations.^{3,5,8,39} Rearranging eq 8, the induced dipole moments can be obtained exactly by inverting the polarization matrix of dimension $3N \times 3N$:

$$\bar{\boldsymbol{\mu}} = (\boldsymbol{\alpha}^{-1} - \mathbf{T}_{(2)}^{\text{tot}})^{-1} \cdot \bar{\mathbf{E}}^{\circ} \quad (9)$$

Equation 9 yields the exact results of the induced dipoles at a given geometry; however, it is rarely used in molecular dynamics simulations⁸ because the computational cost of matrix inversion scales as N^3 , which quickly becomes intractable for large systems. It is, nevertheless, useful for validating the performance and accuracy of other alternatives.

In practice, eq 8 is often solved iteratively until self-consistency is reached. Thus, we start with an initial guess of zero induction, or with a set of induced dipoles from the previous molecular dynamics step:

$$\begin{aligned} \bar{\boldsymbol{\mu}}^{(0)} &= \boldsymbol{\alpha} \cdot \bar{\mathbf{E}}^{\circ} \\ \bar{\boldsymbol{\mu}}^{(1)} &= \boldsymbol{\alpha} \cdot (\bar{\mathbf{E}}^{\circ} + \mathbf{T}_{(2)}^{\text{tot}} \cdot \bar{\boldsymbol{\mu}}^{(0)}) \\ \bar{\boldsymbol{\mu}}^{(n)} &= \boldsymbol{\alpha} \cdot (\bar{\mathbf{E}}^{\circ} + \mathbf{T}_{(2)}^{\text{tot}} \cdot \bar{\boldsymbol{\mu}}^{(n-1)}) \end{aligned} \quad (10)$$

The induced dipoles are considered to be converged when the change of the induced dipoles or the change in the total energy between the previous iteration and the current iteration is smaller than a given threshold criterion. In eq 10, since the intermediate induced dipoles at each iteration are obtained by matrix products over atomic interaction sites, this procedure is called the *direct iterative* approach to be distinguished with the *coupled polarization-matrix inversion and iteration* method described below.

A practical issue is the convergence of the induced dipoles. For short-range interactions between two induced point-dipoles, the TID model yields infinite polarization as the distance between the two interacting sites approaches $(4\alpha_i\alpha_j)^{1/6}$, the so-called polarization catastrophe.²³ In the original paper, Thole considered a number of schemes to reduce short-range interactions,²³ and we choose to employ his second function, corresponding to an exponential charge distribution described by

$$\rho(u_{ij}) = \frac{3b}{4\pi} e^{-bu_{ij}^3} \quad (11)$$

where b is a unitless parameter specifying the screening length with a value of 0.572,²³ and $u_{ij} = r_{ij}/(\alpha_i\alpha_j)^{1/6}$, which depends on the polarizabilities of the two interacting sites. Then, the damped first- and second-order interaction tensors are given below²³

$$\mathbf{T}_{(1)}^{ij,D} = [1 - \exp(-bu_{ij}^3)] \mathbf{T}_{(1)}^{ij} \quad (12)$$

and

$$\mathbf{T}_{(2)}^{ij,D} = \nabla \mathbf{T}_{(1)}^{ij,D} \quad (13)$$

where the superscript D indicates that the interaction tensors have been modified by the damping function shown in eq 12. The damped interaction tensors are used in all calculations; for convenience, the superscript D will be omitted in the rest of the paper unless it is necessary to make this distinction explicitly.

It is of interest to consider a special case in which all N atoms of the system belong to a single molecule. Then, the quantity

$$\mathbf{A} = (\boldsymbol{\alpha}^{-1} - \mathbf{T}_{(2)}^{\text{tot}})^{-1} \quad (14)$$

is a $3N \times 3N$ molecular polarizability tensor distributed over atomic sites. Equation 14 can be reduced to the 3×3 molecular representation, the familiar molecular polarizability tensor $\boldsymbol{\alpha}^{\text{M}}$ with its matrix elements defined by

$$\alpha_{\beta\gamma}^{\text{M}} = \sum_{i=1}^N \sum_{j=1}^N A_{\beta\gamma}^{ij} \quad (15)$$

where the subscripts β and γ specify a Cartesian coordinate

axis respectively. Equation 15 is the definition of molecular polarizability tensor in the Thole interaction dipole model.^{23,24,38} Importantly, anisotropic molecular polarizability can be obtained with the input of only isotropic atomic polarizabilities (atomic parameters $\{\alpha_i; i = 1, N\}$) and the molecular geometry as defined by the second-order interaction tensor $\mathbf{T}_{(2)}^{\text{tot}}$.

III. Coupled Polarization-Matrix Inversion and Iterative (CPII) Method

Unfortunately, even when the interaction tensors are severely damped in the chemical bonding range in the TID model, there is still no guarantee of convergence in the iterative procedure. In fact, we have noticed oscillatory behavior in solving eq 10 for the induced dipole moments, and they become divergent for liquid *N*-methylacetamide and for the (Ala)₅ oligopeptide when intramolecular interactions are included. This is mainly caused by short-range, intramolecular interactions although the chemical bond lengths are greater than the critical distance of polarization catastrophe.²³ Thus, 1–2 and 1–3 intramolecular terms are often excluded in some polarizable models, but they are important in the TID method to obtain the correct molecular polarizability. Here, we present a coupled procedure that employs polarization-matrix inversion for intramolecular interactions and the iterative scheme for intermolecular interactions to achieve the induced dipole convergence of condensed systems.

We first rewrite eq 8 in terms of molecular blocks as follows

$$\bar{\boldsymbol{\mu}}_K = \boldsymbol{\alpha}_K \cdot [\bar{\mathbf{E}}_K^{\circ} + \sum_{L=1}^M \mathbf{T}_{(2)}^{KL} \cdot \bar{\boldsymbol{\mu}}_L]; \quad K = 1, \dots, M \quad (16)$$

where M is the total number of molecules and the vectors and matrices representing induced point dipoles, atomic polarizabilities, atomic partial charges, and the first- and second-order interaction tensors have been grouped into molecular blocks, specified by K and L . Thus, for a water molecule, $\boldsymbol{\mu}_K$ is a vector of nine elements, and for NMA it has a dimension of 36 elements for a total of 12 interaction sites (atoms). Note that the summation in eq 16 includes intramolecular interactions. Equation 16 can be rearranged to yield the expression:

$$\bar{\boldsymbol{\mu}}_K = \mathbf{A}_K \cdot [\bar{\mathbf{E}}_K^{\circ} + \sum_{L \neq K}^M \mathbf{T}_{(2)}^{KL} \cdot \bar{\boldsymbol{\mu}}_L]; \quad K = 1, \dots, M \quad (17)$$

where $\mathbf{A}_K = [\boldsymbol{\alpha}_K^{-1} - \mathbf{T}_{(2)}^{KK}]^{-1}$ is the polarizability tensor for molecule K expressed in terms of distributed atomic sites (eq 14),^{23,24,38} and the permanent electric field $\bar{\mathbf{E}}_K^{\circ}$ includes contributions from all atomic charges including those from molecule K , except 1–2 and 1–3 interactions.

The main advantage of this expression is that eq 17 separates intra- and intermolecular induced dipole interactions, which is essentially a preconditioning procedure and naturally leads to an efficient computational algorithm such that the polarization effects due to intramolecular interactions and due to all other molecules can be computed by different procedures separately. For the intramolecular term, which is primarily responsible for the convergence difficulty in liquid simulations, we explicitly invert the polarization interaction matrix to yield the molecular polarizability for molecule K . Then, the effects of mutual polarization due to all induced dipoles on other molecules ($L \neq K$), as well as the total permanent electric field, are optimized by the computationally efficient, iterative procedure. For a given geometry during molecular dynamics or Monte Carlo simulations, we first obtain the instantaneous molecular polarizabilities $\{\mathbf{A}_K; K = 1, \dots, M\}$, where M is the number of molecules in the

system, by inverting M matrices that have small dimensions and have little effect on the computation scalability in the overall iterative procedure. Then, these molecular polarizability tensors are used to optimize the induced dipoles by looping over the molecular index until self-consistency is achieved.

It is straightforward to apply eq 17 to simple liquids, such as the two systems we consider in this work, liquid water and NMA, in which individual molecules are not covalently linked. For biopolymers such as proteins in which amino acid residues are covalently connected, if we treat each amino acid as an individual “molecule” or fragment indexed by K in eq 17, we still must consider short-range electrostatic and induced-dipolar interactions involving 1–2, 1–3, and 1–4 connections between neighboring residues. In this case, we incorporate a buffered approach to include the explicit short-range interaction. Thus, for residue K , we obtain a polarization matrix that includes the two neighboring residues $K \pm 1$ (of course, only $K + 1$ or $K - 1$ will be included for the two terminal residues), and has a dimension spanning the length of three residues. We label the dimension defined by the three residues $K - 1$, K , and $K + 1$ by the short-hand notation K_{\pm} , and the inverse of the polarization matrix, $\mathbf{A}(K_{\pm})$, for these three residues is explicitly given below:

$$\mathbf{A}(K_{\pm}) = [\boldsymbol{\alpha}_{K_{\pm}}^{-1} - \mathbf{T}_{(2)}^{K_{\pm}K_{\pm}}]^{-1}; \quad K = 1, \dots, M \quad (18)$$

The induced atomic dipoles for residue K are determined from the expression for all three residues:

$$\bar{\boldsymbol{\mu}}_{K_{\pm}} = \mathbf{A}(K_{\pm}) \cdot [\bar{\mathbf{E}}_{K_{\pm}}^{\circ} + \sum_{L \neq K_{\pm}}^M \mathbf{T}_{(2)}^{K_{\pm}L} \cdot \bar{\boldsymbol{\mu}}_L] \quad (19)$$

Note that the symbol K_{\pm} indicates that the associated matrices have dimensions defined by residues $K - 1$, K , and $K + 1$, except when K is a terminal residue in which case there is only one buffer residue. It is important to point out that eq 19 is used to compute the induced atomic dipole moments only for residue K , which is updated for the iterative process. Although the expression in eq 19 also yields induced dipoles for residues $K - 1$ and $K + 1$, they are not enumerated nor used since they are treated in exactly the same manner as that for residue K . Consequently, as the loop over residue in the algorithm moves to the next residue, $K + 1$, residue K becomes a buffer, and finally it takes the role of an external field for residue $K + 2$. Although it appears that the neighboring buffer approach increases the computational efforts slightly because a larger polarization matrix is diagonalized, the overall computational costs in fact are significantly decreased because the induced dipoles are easily converged with fewer iteration steps, and the dimension for the three-residue polarization matrix is still very small compared with the size of a solvated protein system.

IV. Results and Discussion

The coupled polarization-matrix inversion and iteration (CPII) method has been implemented in the CHARMM program.⁴⁰ To illustrate the performance of the computational algorithm, we have applied the CPII method to three systems, including a box of 4096 water molecules, a box of 2048 NMA molecules,²⁶ and a pentaalanine peptide (Ala)₅. The first two systems are treated by periodic boundary conditions along with particle mesh Ewald summation to incorporate long-range electrostatic interactions both from the permanent partial atomic charges^{41,42} and from the induced dipole moments.⁴³ The purpose of this calculation is to show the convergence behavior of the CPII method compared with the direct iterative approach with and without the inclusion of short-range intramolecular interactions in the Thole interaction

TABLE 1: Isotropic Atomic Polarizability Parameters for Each Element (in Å³)

atom	$\bar{\alpha}$
H	0.496
C	1.334
N	1.073
O	0.837

TABLE 2: Computed Anisotropic and Average Isotropic Molecular Polarizabilities (in Å³) for Water and *N*-Methylacetamide (NMA) Using the Thole Interaction Dipole Model That Includes All Intramolecular Pair Interactions and That Excludes Short-Range 1–2 through 1–4 Atom-Connectivities

molecule	$\bar{\alpha}^M$	α_{xx}^M	α_{yy}^M	α_{zz}^M
water	1.41	1.32	1.80	1.12
excl. 1–2 pairs	1.86	1.71	2.16	1.71
excl. 1–2 and 1–3 pairs	1.83	1.83	1.83	1.83
MP2/6-31G(+sd+sp) ⁴⁷	1.33	1.32	1.44	1.24
exptl ⁴⁵	1.47	1.47	1.53	1.42
NMA	7.81	9.84	7.68	5.90
excl. 1–2 pairs	10.16	13.43	9.25	7.81
excl. 1–2 and 1–3 pairs	9.59	11.22	9.01	8.55
excl. 1–2, 1–3 and 1–4 pairs	9.47	10.16	9.22	9.03
MP2/6-31++G(d,p) ⁴⁴	7.23	8.80	7.49	5.41
exptl ⁴⁶	7.82			

dipole model. Thus, we have taken a configuration from our previous molecular dynamics simulations of liquid water and NMA,²² which is as a random selection as any configurations generated from the dynamics simulation. We note that the dipole convergence problem also exists in other configurations saved from the trajectories generated by using the CPII method. Thus, the numerical instability is not simply due to a rare structure of the liquid systems. For (Ala)₅, an optimized linear conformation of the pentapeptide was employed. The atomic coordinates for small systems are provided as Supporting Information and the isotropic atomic polarizabilities^{23,24,26} used in the present study are given in Table 1.

It is of interest to first examine the static molecular polarizabilities for water and NMA determined by including all intramolecular induced dipole–induced dipole interactions, and by selectively excluding short-range interactions that involve atoms bonded covalently (called 1–2 interactions), that form bond angles (called 1–3 interactions), and that participate in torsional interactions (called 1–4 interactions). Note that in the standard CHARMM22 force field,²³ 1–2 and 1–3 atom pairs are excluded from electrostatic interactions due to the permanent partial charges. The computed anisotropic molecular polarizabilities and the average isotropic molecular polarizabilities are summarized in Table 2 along with the experimental data and ab initio MP2 results.

First, the computed average (isotropic) molecular polarizabilities for water and NMA are in excellent agreement with experiment only when all intramolecular interactions are included. In fact, one of the most attractive features of the TID model is that an excellent agreement between computed and experimental molecular polarizabilities can be obtained for a wide range of organic compounds using a single set of isotropic atomic polarizability parameters (Table 1).^{23,24} This is in contrast with other polarizable force fields in which different atomic polarizability parameters are required for the same element in different functional groups^{8–22,44} and sometimes isotropic atomic polarizabilities²⁰ are used. However, when 1–2 and 1–3 atom pairs are excluded in water, the computed average molecular

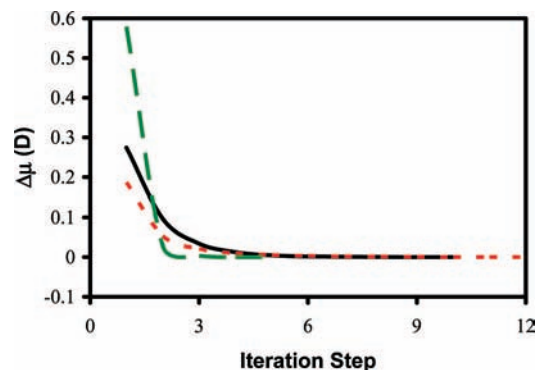


Figure 1. The variation in mean induced dipole moment $\Delta\mu$ (D/atom) between successive iteration steps (eq 20), using the coupled polarization-matrix inversion and iteration (CPII) method for a cubic box of 4096 water molecules (solid line in black), a cubic box consisting of 2048 *N*-methylacetamide (NMA) molecules (dotted line in red), and an optimized linear conformation of alanine pentapeptide (dashed line in green). Convergence criterion is 0.0001 D/atom between two successive iteration steps over the molecular index.

polarizability is overestimated by as much as 30%,⁴⁵ whereas for NMA, in which the 1–4 interaction exclusion is also considered, the average molecular dipole polarizability is overestimated by 21–30%.⁴⁶ Thus, it is necessary to include all atomic pair interactions in the TID model.

Second, it is important to note that although isotropic atomic polarizability tensors are used, the TID model is capable of yielding anisotropic molecular polarizabilities. The comparison of the diagonal elements of the TID anisotropic polarizability tensor is best made with *ab initio* results since it is difficult to obtain reliable experimental data. In general, the use of a large basis set with diffuse functions and electron correlations are essential in these calculations; still, at the MP2/6-31G(+sd+sp) level of theory,⁴⁷ the computed molecular polarizability for water is underestimated by 10% in comparison with experiment, and that for NMA with the 6-31++G(d,p) basis set is about 8% less than the experimental value.⁴⁴ Nevertheless, comparison of the relative anisotropic components can give a good assessment of the corresponding values obtained with the TID model. For water, the principal axis *y* is placed along the C_2 axis in the direction away from the hydrogen atoms and *z* is made perpendicular to the molecular plane. The TID model yields (a_{xx}^M , a_{yy}^M , a_{zz}^M) values of (1.32, 1.80, 1.12) Å³, which may be compared with the experimental data of (1.47, 1.53, 1.42) Å³.⁴⁵ The corresponding MP2 results are (1.32, 1.44, 1.24) Å³.⁴⁷ In all cases, the polarization along the principal axis is the largest anisotropic component. For NMA, whose coordinate system is chosen as the standard orientation as in the Gaussian program, the computed anisotropic polarizabilities are (9.84, 7.68, 5.90) Å³ from the TID model, compared with the MP2 values of (8.80, 7.49, 5.41) Å³.⁴⁴ The trends and relative magnitude of the three main anisotropic polarizability components are in good accord between the TID model and *ab initio* MP2 results. This is particularly remarkable in view of the fact that just a single isotropic polarizability is used for each element (Table 1). When short-range intramolecular interactions are excluded, the computed anisotropy becomes less distinctive; for example, the three components (a_{xx}^M , a_{yy}^M , a_{zz}^M) are identical for water with a value of 1.83 Å³ without intramolecular interactions, and the three components for NMA are (10.16, 9.22, 9.03) Å³. This further emphasizes that it is necessary to include all intramolecular terms in the TID model.

For systems consisting of a collection of polarizable molecules such as simple liquids or polypeptides, the mutual polarization

TABLE 3: Computed Monomer Polarization Energies (kcal/mol) for Water and *N*-Methylacetamide in a Liquid Configuration and in the Gas Phase with and without the Inclusion of Induction Interactions from Intramolecular 1–2, 1–3, and 1–4 Atomic Pairs

molecule	liquid	gas	difference
water	−4.63	0.00	−4.63
excl. 1–2 and 1–3 pairs	−5.47	0.00	−5.47
NMA	−6.43	−5.03	−1.40
excl. 1–2, 1–3, and 1–4 pairs	−3.62	−1.13	−2.49

of all polarizable sites at a given configuration is typically determined by an iterative process depicted in eq 10 since it is impractical to invert a large polarization matrix at every time step during a molecular dynamics simulation or every Monte Carlo move. Thus, the computational efficiency is directly related to the number of iterations needed to achieve convergence at a given error tolerance. This is particularly true in molecular dynamics simulations because only when induced dipole moments are converged to sufficient accuracy can energy gradient be calculated accurately and energy conservation be maintained. In the present calculation, we use a dipolar convergence tolerance of 0.0001 D/atom for the average change in induced dipole moment between successive iteration steps:

$$\Delta\mu^{(n)} = \left[\frac{1}{3N} \sum_{i=1}^N \sum_{\beta} (\mu_{i\beta}^{(n)} - \mu_{i\beta}^{(n-1)})^2 \right]^{1/2} \leq 0.0001 \text{ D} \quad (20)$$

where $\{\beta \in x, y, z\}$ and N is the total number of polarizable sites.

The mean variation in induced dipole moment between successive iteration steps, $\Delta\mu^{(n)}$, employing the CPII method is displayed in Figure 1, and the number of iterations needed to reach this convergence tolerance is 10, 13, and 5 steps for a box of 4096 water molecules, a box of 2048 NMA molecules, and one pentapeptide (Ala)₅ molecule, starting with zero-induction. We note that the polarization-matrix inversion in eqs 17 and 18 is local for a monomer molecule in the liquid or a tripeptide unit for (Ala)₅ and only needs to be performed once during the iterative process for each given geometrical configuration. In the two liquid cases, periodic boundary conditions are used along with the particle mesh Ewald method for long-range electrostatic interactions. At this convergence tolerance (0.0001 D/atom), the computed polarization energies are −4.63 and −6.43 kcal/mol per monomer for liquid water and NMA, respectively (Table 3). It should be pointed out that since the permanent electric fields originating from atoms within two chemical bonds do not contribute to intramolecular dipole inductions, the net polarization for an isolated water molecule in the gas phase is zero. For larger molecules such as NMA, the situation is quite different. The electric fields from distant partial charges within the same molecule induce point-dipole polarization, and the resulting induced fields will interact with and enhance dipole induction at all polarizable sites including those chemically bonded. The self-induction polarization energy is −5.03 kcal/mol for an isolated NMA molecule in the gas phase. Thus, intermolecular interactions in the liquid phase further enhance polarization energy by −1.40 kcal/mol (Table 3).

The convergence behaviors for the induced dipoles using the direct iterative approach are shown in Figure 2. In the first case, when all intramolecular interactions are included, all three systems show an initial decrease in dipole induction, but both liquid NMA and alanine pentapeptide exhibit rapid divergence

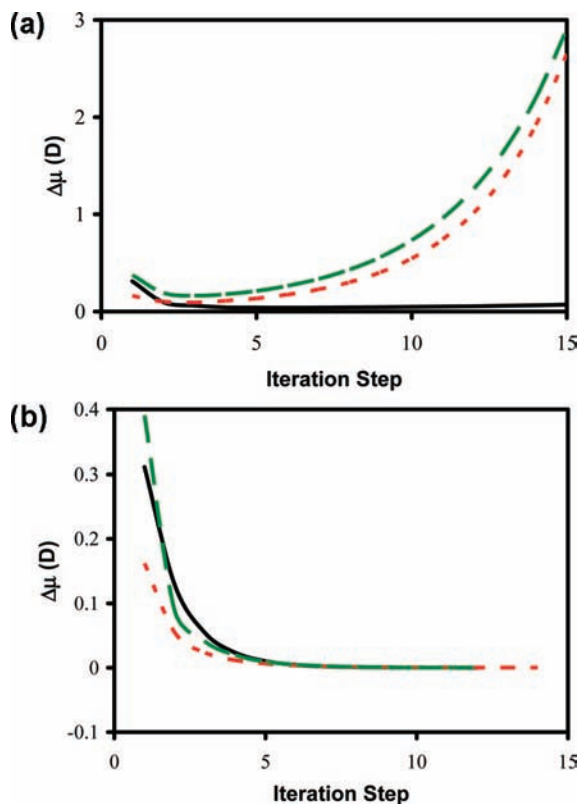


Figure 2. The variation in mean induced dipole moment $\Delta\mu$ (D/atom) between successive iteration steps, using the direct iterative self-consistent-field approach for a cubic box of 4096 water molecules (solid line in black), a cubic box consisting of 2048 *N*-methylacetamide (NMA) molecules (dotted line in red), and an optimized linear conformation of alanine pentapeptide (dashed line in green): (a) all intramolecular pair interactions are included in the direct iterative procedure with which the induced dipole moments failed to converge for all three cases and (b) convergence in induced dipole moment is achieved when 1–2, 1–3, and/or 1–4 intramolecular interactions are excluded. The same coordinate configurations are used as those illustrated in Figure 1. Convergence tolerance is set at 0.0001 D/atom between two successive iteration steps.

in induced polarization, whereas oscillation in the computed induced dipoles is observed for liquid water without reaching the convergence tolerance within 15 iterative steps (Figure 2a). When short-range, intramolecular induced-dipole interactions up to 1–4 bonded pairs are excluded from the interaction tensors $\mathbf{T}_{(n)}^{\text{tot}}$, $n = 1$ and 2, dipole convergence by direct iteration can be obtained in all three cases (Figure 2b). A total of 12, 14, and 12 iteration steps are needed for the water, NMA, and (Ala)₅ system, respectively. On the basis of this observation, we conclude that the divergence of induced dipole can be attributed to short-range (1–2, and 1–3) interactions that lead to numerical instability.

The total induced polarization energies are -5.47 and -3.62 kcal/mol for the same water and NMA liquid configurations

(Table 3). In this case, the polarization energy for water is greater than that from the CPII method because the molecular polarizability $\bar{\alpha}^M$ without 1–2 and 1–3 interactions is 30% greater than that when full intramolecular interactions are included in the second-order dipolar interaction tensor (Table 2). For NMA, although the polarization energy, excluding 1–2 through 1–4 induction interactions, appears to be smaller than that from the CPII model (Table 3), the interaction polarization energy, which is the difference of polarization energies in the liquid and in the gas phase, actually is greater because the self-induction energy is much smaller for an isolated NMA molecule in the gas phase (-1.13 kcal/mol) than the case where all intramolecular induction interactions are included (-5.03 kcal/mol). Recall that it is necessary to include all intramolecular interactions in the TID model, including chemically bonded atom pairs, in order to adequately describe the total molecular polarization as measured by the anisotropic molecular polarizability tensor. The exclusion of 1–2 through 1–4 induction interactions can have significant effects on polarization interactions; in fact, it represents a different polarization model.

Finally, we turn our attention to the total CPU time needed for different methods. We again stress that in the present CPII scheme, the required polarization-matrix inversion for each molecular or residue fragment is only calculated once, which is then stored in the memory. The self-consistent-field (SCF) iteration process is carried out by looping over molecules and residues in the system (eqs 17 and 19). On the other hand, in the direct iterative process, the induced dipoles are successively enumerated over atomic interaction sites (eq 10). Note that the total computing costs are similar in each iteration for the two numerical loops because the number of polarizable sites is the same. At full convergence, the two schemes yield identical results; however, in the present test case, the direct iterative procedure failed to converge if all intramolecular interactions are included. Thus, in practice, the final converged induction energy by direct iteration that excludes bonded intramolecular interactions is not identical with that obtained by using the CPII method.

Table 4 shows the CPU time required for inverting 4096 polarization matrices for the water system and 2048 polarization matrices for the NMA system, for one iteration over molecular index, and the total CPU cost for obtaining the fully converged induced dipoles at a tolerance of 0.0001 D/atom with the CPII method. In addition, the CPU times needed for one iteration and for full convergence using the direct iteration procedure are also given. In the case of liquid water, the CPU time for matrix inversion is only 4% of CPU time for the first iteration step, while for liquid NMA, the CPU time for matrix inversion is about 15% of the time spent in one iteration because a greater matrix is needed for the NMA molecule (36×36 for NMA vs 9×9 for water). There is no additional CPU time required for matrix inversion in subsequent SCF steps since the instantaneous molecular polarizability tensors are saved in the memory. Thus, the percentage of CPU time spent on matrix inversion is

TABLE 4: CPU Time (in s) Spent on Matrix Inversion, One Self-Consistent-Field Iteration, and Fully Converged Induction, Using the Coupled Polarization-Matrix Inversion and Iteration (CPII) Method and the Direct Iteration Approach^a

system	CPII			direct iteration	
	matrix inv.	1 iteration	total	1 iteration	total
water (4096 monomers)	0.040	0.966	9.700	0.966	11.59
NMA (2048 monomers)	0.389	2.198	28.96	2.138	29.93

^a Long-range electrostatic effects both from the permanent partial charges and the induced dipole moments are treated by the particle-mesh Ewald method.

negligible compared with the total CPU time needed to achieve full polarization convergence in the CPII method.

In comparison with the direct iterative method, the CPII method shows slight improvement in convergence speed, reducing two SCF iterations for one configuration of a cube of water, and by one SCF iteration for a box of liquid NMA. The improvement is more noticeable in the case of alanine pentapeptide, in which the number of SCF iterations is reduced from 12 to 5, keeping in mind that the direct iterative approach excludes intramolecular interactions up to 1–4 pairs, whereas all terms are included in the CPII method. However, we point out that this comparison is not based on equivalent procedures. First, the induced dipoles do not converge in our implementation of the Thole model when 1–2, 1–3, and 1–4 intramolecular terms are included as they are required due to numerical instability in the iterative process. The CPII method allows us to achieve dipole convergence using the Thole model with all intramolecular interactions. The preconditioning CPII approach is applicable to other polarization force field models. We note that there are other ways such as the polarization cutoff approach²⁷ for the short interatomic distance to remedy polarization convergence difficulties and to accelerate computational speed. Second, to obtain “converged” results, we have to remove short-range intramolecular dipolar interactions. This reduces the number of numerical operations, and removes the closest interaction terms that contribute the most to intramolecular polarization, which would have increased the number of iterations had it converged. Thus, the total amount of CPU time needed to converge the induced dipoles may be reduced more than that indicated in Table 4.

V. Conclusion

We have described a coupled polarization-matrix inversion and iteration (CPII) method to achieve convergence in induced dipole moments and to reduce the number of self-consistent-field iterations for liquid and polypeptide systems employing a polarizable intermolecular potential function (PIPF) based on the Thole interaction dipole (TID) model. The Thole interaction dipole model was designed to yield anisotropic molecular polarizability by using isotropic atomic polarizability parameters, in which all atomic pair interactions are considered, including those that are directly bonded covalently. To avoid polarization catastrophe when two polarizable sites approach a distance of $(4\alpha_i\alpha_j)^{1/6}$ in classical polarization models, short-range interactions are severely damped by using an exponential function that greatly reduces the interaction tensors near the chemical bonding distances. The TID model can yield excellent results in the average isotropic and anisotropic molecular polarizabilities in comparison with experimental data and results from ab initio MP2/6-31++G(d,p) calculations. We found that it is critical to include all intramolecular pair interactions in the interaction tensor to describe the anisotropy of molecular polarization, whereas it is inadequate if intramolecular induced-dipole terms (1–2, 1–3, and 1–4 interactions) are excluded as is typically done in molecular mechanics force fields.

For condensed phase systems and polypeptides, converged induced dipoles can be obtained either by inverting a $3N \times 3N$ polarization-matrix where N is the number of polarizable sites, or by an iterative self-consistent-field (SCF) approach. The direct iterative SCF approach is more efficient computationally for large systems and is typically used in molecular dynamics simulations. We found that induced dipole moments failed to converge by the direct iterative approach if 1–2, 1–3, and 1–4 intramolecular interactions are included in the dipolar interaction

tensor as is required in the Thole model to correctly model the anisotropy of molecular polarization. To solve this numerical stability problem, we reformulated the Thole interaction dipole model in terms of molecular block-matrices, which naturally leads to a coupled algorithm that involves a polarization-matrix inversion term to account for intramolecular interactions, and an iterative procedure to incorporate the mutual polarization effects between different molecules. This coupled approach avoids the numerical instability for short-range interactions by obtaining their mutual polarization exactly. The CPII method is illustrated by applying it to two cubic boxes of water and NMA molecules as well as an alanine pentapeptide configuration whose coordinates were generated from previous molecular dynamics simulations or by energy minimization. It is shown that the CPII method can achieve convergence for the dipole induction polarization rapidly in all cases, whereas the direct iterative approach failed to reach convergence in these cases. In addition, the CPII reduces the overall computational costs by decreasing the number of iteration steps in comparison with the direct iteration approach that excludes intramolecular bonded interactions.

Acknowledgment. This work is supported by the National Institutes of Health (GM46736).

Supporting Information Available: Listing of Cartesian coordinates for small systems used in the calculations. This material is available free of charge via the Internet at <http://pubs.acs.org>.

References and Notes

- (1) For the summary of a special issue on polarization, see: Jorgensen, W. L. *J. Chem. Theory Comput.* **2007**, *3*, 1877.
- (2) Ponder, J. W.; Case, D. A. *Adv. Protein Chem.* **2003**, *66*, 27.
- (3) Vesely, F. J. *J. Comput. Phys.* **1977**, *24*, 361.
- (4) Stillinger, F. H.; Weber, T. A.; David, C. W. *J. Chem. Phys.* **1982**, *76*, 3131.
- (5) Van Belle, D.; Couplet, I.; Prevost, M.; Wodak, S. J. *J. Mol. Biol.* **1987**, *198*, 721.
- (6) Niesar, U.; Corongiu, G.; Clementi, E.; Kneller, G. R.; Bhattacharya, D. K. *J. Phys. Chem.* **1990**, *94*, 7949.
- (7) Sprik, M.; Klein, M. L.; Watanabe, K. *J. Phys. Chem.* **1990**, *94*, 6483.
- (8) Ding, Y.; Bernardo, D. N.; Krogh-Jespersen, K.; Levy, R. M. *J. Phys. Chem.* **1995**, *99*, 11575.
- (9) Gao, J.; Habibollahzadeh, D.; Shao, L. *J. Phys. Chem.* **1995**, *99*, 16460.
- (10) Gao, J.; Pavelites, J. J.; Habibollahzadeh, D. *J. Phys. Chem.* **1996**, *100*, 2689.
- (11) (a) Dang, L. X.; Chang, T.-M. *J. Chem. Phys.* **1997**, *106*, 8149. (b) Caldwell, J. W.; Kollman, P. A. *J. Phys. Chem.* **1995**, *99*, 6208. (c) Cieplak, P.; Caldwell, J.; Kollman, P. *J. Comput. Chem.* **2001**, *22*, 1048.
- (12) Rick, S.; Stuart, S.; Berne, B. *J. Chem. Phys.* **1994**, *101*, 6141.
- (13) Stern, H. A.; Kaminski, G. A.; Banks, J. L.; Zhou, R.; Berne, B. J.; Friesner, R. A. *J. Phys. Chem. B* **1999**, *103*, 4730.
- (14) Patel, S.; Brooks, C. L. *J. Comput. Chem.* **2004**, *25*, 1.
- (15) Patel, S.; Mackerell, A.; Brooks, C. *J. Comput. Chem.* **2004**, *25*, 1504.
- (16) Patel, S.; Brooks, C. L., III *J. Chem. Phys.* **2005**, *123*, 164502.
- (17) Sprik, M.; Klein, M. L. *J. Chem. Phys.* **1998**, *89*, 7556.
- (18) Lamoureux, G.; Roux, B. *J. Chem. Phys.* **2003**, *119*, 3025.
- (19) Lamoureux, G.; Alexander, D.; Mackerell, J.; Roux, B. *J. Chem. Phys.* **2003**, *119*, 5185.
- (20) Harder, E.; Anisimov, V. M.; Vorobyov, I. V.; Lopes, P. E. M.; Noskov, S. Y.; MacKerell, A. D., Jr.; Roux, B. *J. Chem. Theory Comput.* **2006**, *2*, 1587.
- (21) Anisimov, V. M.; Vorobyov, I. V.; Roux, B.; MacKerell, A. D., Jr. *J. Chem. Theory Comput.* **2007**, *3*, 1927.
- (22) Harder, E.; Anisimov, V. M.; Whitfield, T.; MacKerell, A. D., Jr.; Roux, B. *J. Phys. Chem. B* **2008**, *112*, 3509.
- (23) Thole, B. T. *J. Chem. Phys.* **1981**, *59*, 341.
- (24) van Duijn, P. Th.; Swart, M. *J. Phys. Chem. A* **1998**, *102*, 2399.
- (25) Bernardo, D. N.; Ding, Y.; Krogh-Jespersen, K.; Levy, R. M. *J. Comput. Chem.* **1995**, *16*, 1141.

- (26) Xie, W.; Pu, J.; Mackerell, A. D., Jr.; Gao, J. *J. Chem. Theory Comput.* **2007**, *3*, 1878.
- (27) Kaminski, G. A.; Friesner, R. A.; Zhou, R. *J. Comput. Chem.* **2003**, *24*, 267.
- (28) Kaminski, G. A.; Stern, H. A.; Berne, B.; Friesner, R. A. *J. Phys. Chem. A* **2004**, *108*, 621.
- (29) Ren, P.; Ponder, J. W. *J. Comput. Chem.* **2002**, *23*, 1497.
- (30) Ren, P.; Ponder, J. W. *J. Phys. Chem. B* **2003**, *107*, 5933.
- (31) Gao, J. *J. Phys. Chem. B* **1997**, *101*, 657.
- (32) Gao, J. *J. Chem. Phys.* **1998**, *109*, 2346.
- (33) Wierzbowski, S. J.; Kofke, D. A.; Gao, J. *J. Chem. Phys.* **2003**, *119*, 7365.
- (34) Xie, W.; Gao, J. *J. Chem. Theory Comput.* **2007**, *3*, 1890.
- (35) Xie, W.; Song, L.; Truhlar, D.; Gao, J. *J. Chem. Phys.* **2008**, *128*, 234108.
- (36) Xie, W.; Song, L.; Truhlar, D.; Gao, J. *J. Phys. Chem. B* **2008**, *112*, 14124.
- (37) MacKerell, A. D., Jr.; Bashford, D.; Bellott, M.; Dunbrack, R. L., Jr.; Evanseck, J. D.; Field, S.; Fischer, M. J.; Gao, J.; Guo, H.; Ha, S.; Joseph-McCarthy, D.; Kuchnir, L.; Kuczera, K.; Lau, F. T. K.; Mattos, C.; Michnick, S.; Ngo, T.; Nguyen, D. T.; Prodhom, B.; Reiher, W. E., III; Roux, B.; Schlenkrich, M.; Smith, J. C.; Stote, R.; Straub, J.; Watanabe, M.; Wiorkiewicz-Kuczera, J.; Yin, D.; Karplus, M. *J. Phys. Chem. B* **1998**, *102*, 3586.
- (38) Applequist, J.; Carl, J. R.; Fung, K. *J. Am. Chem. Soc.* **1972**, *94*, 2952.
- (39) Kolafa, J. *J. Comput. Chem.* **2004**, *25*, 335.
- (40) Brooks, B. R.; Brucocoli, R. E.; Olafson, B. D.; States, D. J.; Swaminathan, S.; Karplus, M. *J. Comput. Chem.* **1983**, *4*, 187.
- (41) Darden, T.; York, D. M.; Pedersen, L. G. *J. Chem. Phys.* **1993**, *98*, 10089.
- (42) Essmann, U.; Perera, L.; Berkowitz, M. L.; Darden, T.; Lee, H.; Pedersen, L. G. *J. Chem. Phys.* **1995**, *103*, 8577.
- (43) Toukmaji, N.; Sagui, C.; Board, J.; Darden, T. *J. Chem. Phys.* **2000**, *113*, 10913.
- (44) Mannfors, B.; Mirkin, N. G.; Palmo, K.; Krimm, S. *J. Comput. Chem.* **2001**, *22*, 1933.
- (45) Murphy, W. F. *Chem. Phys.* **1981**, *59*, 341.
- (46) D'Alelio, G. F.; Reid, E. E. *J. Am. Chem. Soc.* **1937**, *59*, 109.
- (47) Maple, J. R.; Ewig, C. S. *J. Chem. Phys.* **2001**, *115*, 4981.

JP808952M